EASR

Engineering and Applied Science Research

https://www.tci-thaijo.org/index.php/easr/index

Published by the Faculty of Engineering, Khon Kaen University, Thailand

Variations in acoustic emission characteristics across different deformation stages of various materials

Atip Loetpiya[1)], Patamaporn Chaikool[2)], Yoshiharu Mutoh[3)], Prinya Chindaprasirt[4, 5)] and Teerawat Laonapakul*[1)]

[1)]Department of Industrial Engineering, Faculty of Engineering, Khon Kaen University, Khon Kaen 40002, Thailand
[2)]Department of Mechanical Engineering, Faculty of Engineering, Rajamangala University of Technology Isan Khon Kaen Campus, Khon Kaen 40000, Thailand
[3)]Nagaoka University of Technology, Nagaoka, Niigata 940-2188, Japan
[4)]Sustainable Infrastructure Research and Development Center, Department of Civil Engineering, Faculty of Engineering, Khon Kaen University, Khon Kaen 40002, Thailand
[5)]Academy of Science, The Royal Society of Thailand, Bangkok 10300, Thailand

Received 21 November 2024
Revised 24 February 2025
Accepted 27 February 2025

Abstract

Integration of acoustic emission (AE) monitoring with traditional mechanical testing presents an attractive methodology for the prediction and assessment of material failure processes. While AE monitoring during mechanical testing has been extensively applied to study deformation and fracture in individual materials, conducting a comparative analysis across various monolithic materials using a single AE system provides valuable insights. This approach helps identify material-specific signal characteristics and behaviors that are essential for predicting failure in complex, multi-material structures. In this study, uniaxial testing with AE monitoring was conducted for evaluating failure behaviors of four different materials, namely low-carbon steel, aluminum alloy, acrylic and white Portland cement (WPC). The AE patterns obtained from tensile testing of ductile metallic materials, low-carbon steel and aluminum alloy clearly indicated the regions of elastic, plastic and fracture by difference of peak amplitude intensity of AE signals. AE signals obtained from brittle materials, PMMA acrylic and WPC specimens showed fluctuated AE peak amplitude intensities throughout the linear deformation region until specimen fracture. The AE signals and their corresponding Fast Fourier Transform spectra provide data indicating failure of different materials, as well as failure behaviors, i.e., elastic, plastic and fracture, of ductile metallic materials.

Keywords: Acoustic emission waveform, Fast Fourier transformation, Failure behaviors, Metallic materials, Brittle materials

1. Introduction

Standard mechanical testing approaches, such as tension or compression testing, can give the basic characteristics of materials. However, they have some limitations. In particular, they are unable to detect the details of deformation and fracture processes and mechanisms such as plastic deformation, microcracking, void formation, coalescence of void or crack, crack propagation, and final fracture. Combining Acoustic Emission (AE) monitoring or other non-destructive testing with standard mechanical testing would be an interesting approach for predicting and evaluating failure processes. AE monitoring techniques have become accepted as non-destructive testing methods. These techniques hold the potential to predict material failure behaviors during their operational lifespan [1-3]. This is a useful material research approach for monitoring defect development, such as micro- and macro-fractures, as well as structural material failures. AE signals correspond to sound waves released during deformation, nucleation and propagation of cracks in a material due to the development of sudden localized deformations. When any of these failure mechanisms occur in materials, energy is released and part of this energy is scattered in the form of acoustic waves.

The mechanical properties obtained by standard mechanical testing are useful for designing machine parts and structures using as-received materials. However, only mechanical properties are insufficient. Detailed information on deformation and fracture obtained from AE monitoring is essential when parts and structures are fabricated through processes such as stamping [4, 5], bending [6], forming and grinding [7]. Additionally, it is also important to understand the material behavior, especially when it is non-metallic and sensitive to the production process, such as ceramics, acrylic [8, 9], bone cement [10, 11], thermoplastic and thermoset polymeric coatings [12] and calcium phosphate coatings utilized as biomaterials [13, 14]. For the AE analysis, AE signals are detected by a sensor, amplified and then the AE parameters are recorded. AE parameters, such as event count, ring-down count, energy, duration, and amplitude, are commonly used to investigate fracture behavior and the severity of damage during a test [15]. Additionally, Fast Fourier Transform (FFT) analysis serves as a valuable tool in waveform signal processing that helps in understanding the behavior and characteristics of the signals from a frequency-based perspective. This approach is a widely used technique for converting AE signals from the time domain to the frequency domain, enabling extraction of valuable information. The frequency characteristics of AE signals are directly linked to specific damage mechanisms. Various damage modes generate AE signals with distinct frequency profiles,

*Corresponding author.
Email address: teerla@kku.ac.th
doi: 10.14456/easr.2025.19

enabling the identification and differentiation of failure mechanisms [16]. According to the literature, AE monitoring during mechanical testing has been widely used to investigate deformation and fracture processes in individual materials, including metals (e.g., steels [17, 18], aluminum alloys [19, 20]) and non-metals (e.g., acrylic [8, 9], cement mortar [21, 22]). A comparative analysis of various monolithic materials using a single AE system would be beneficial, as inconsistencies in results can arise when different AE systems are employed. By using a single AE system, it would be possible to identify distinct signal differences among various materials, providing valuable insights into their unique characteristics and behaviors. This understanding of AE behavior is crucial for future studies focused on predicting failure in complex, multi-material structures.

The present study conducts a comparative analysis of AE signals generated by various monolithic materials, including low-carbon steel, aluminum alloy, PMMA acrylic, and white Portland cement (WPC), using a standardized AE system. This comprehensive selection offers a more integrated understanding of how different materials behave under stress. The differences in AE signal characteristics and the failure mechanism of each material were examined.

2. Experimental procedures

2.1 Material and specimen preparation

Four types of materials were used in this investigation: low-carbon steel plate (SS400), aluminum alloy plate (Al1100), PMMA acrylic plate and cube-shaped WPC. The selection of these four materials was based on their representation of the major material categories, including ferrous, nonferrous, polymer, and ceramic. The low-carbon steel, aluminum alloy and acrylic plate specimens were prepared according to JIS Z2201 standard guidelines (No. 13-B) for tensile testing [23]. Figure 1 illustrates the shape and dimensions of the dog-bone specimen. The as-received plate thickness of the low-carbon steel, aluminum alloy and acrylic plate is 4, 6 and 3 mm, respectively. These specimens were cut from the as-received plates using a CNC milling machine. The loading direction of the low-carbon steel and aluminum alloy specimens was adjusted to the rolling direction of the plate. WPC pastes were prepared with distilled water at a cement to liquid ratio of 2:1 on a weight basis. The WPC pastes were cast into 25×25×25 mm^3 acrylic cubic moulds for compression testing. Freshly mixed samples were compacted using a vibrating machine for 15 sec to remove entrapped air, then wrapped with plastic sheets and cured in a temperature-controlled chamber at 23 °C for 24 hours. After curing, samples were removed from the moulds and further cured in water for 28 days at room temperature. The cured samples were then dried at 40 °C for 24 hours and stored in a desiccator.

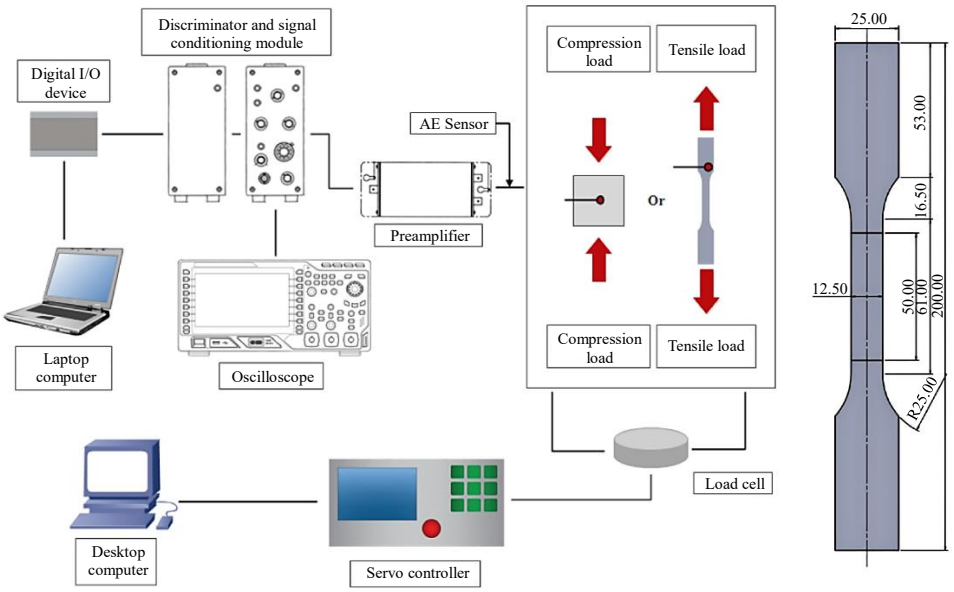

Figure 1 Schematic diagram of experimental setup and AE monitoring system for tensile and compression testing

2.2 Uniaxial (tensile and compression) testing with an acoustics emission monitoring system

A schematic diagram of the experimental setup and AE monitoring system for uniaxial (tensile and compression) testing is illustrated in Figure 1. Uniaxial tests were conducted using a hydraulic testing machine with a load cell of 100 kN capacity under room temperature (25-30 °C). Tensile tests on steel and aluminum alloy were conducted using a loading speed of 0.1 mm/sec. For brittle materials, both the tensile test for PMMA acrylic and the compression test for WPC cement were conducted under a loading speed of 0.01 mm/sec. An AE sensor was attached to the upper side (outside gauge section) of the tensile specimens, as seen in Figure 1. A rubber sheet, 1 mm thick, was placed between the tensile specimen and the machine clamp to eliminate the noise generated by the clamped parts. On the other hand, for the compression specimen, the AE sensor was attached to the center of the cube surface. A small amount of grease was spread on the specimen surface to transfer the elastic wave to the AE sensor. The AE monitoring system was composed of an AE sensor (AE 900M, NF Corporation), preamplifier (AE 912, NF Corporation), discriminator (AE 9922, NF Corporation), signal conditioning module (As-712, NF Corporation), portable digital I/O device (NI USB 6501, National Instruments) and an oscilloscope (DS2302A, RIGOL), as found in Figure 1. The sensor (AE 900M), with wide frequency capabilities ranging from 300 kHz to 2 MHz, was chosen for this study. This wideband sensor enables the detection of AE signals across a wide frequency spectrum, making it particularly beneficial for monitoring materials with diverse failure mechanisms, where AE signals may exhibit varying frequency characteristics. A gain of 20 dB was preset on the discriminator, along with a high pass filter set at 20 kHz and a

threshold value of 0.35 V. The AE system used for AE peak amplitude monitoring had a sampling rate of 1 Hz. Before initiating the test, environmental signals were carefully monitored and controlled to eliminate any potential influence on the test results. AE signals were monitored during the whole test until final fracture for all the specimens to investigate the deformation and failure processes. Ten samples of each material were tested to study the correlation between the stress-time curve and AE behavior. The relationship between the peak amplitude of the detected AE signal and the stress behavior of the samples was obtained to investigate the failure mechanisms of the tested samples. During the tests, raw AE waveforms were recorded at a sampling rate of 1 MHz using an oscilloscope. These time-domain signals were then processed using Fast Fourier Transformation (FFT) to convert them into the frequency domain for analysis. This analysis enables the identification of specific frequency ranges associated with distinct failure mechanisms characteristic of each material.

3. Results and discussion

3.1 Uniaxial testing and AE behavior

Figures 2(a-d) show two examples of AE peak amplitude variations along with the stress-time curves of materials (steel, aluminum alloy, acrylic, and WPC) during uniaxial testing. The AE signals were continuously recorded from the start of initial loading until the final fracture. Variations in AE peak amplitude and pattern were not substantially different for each type of material. The fracture and AE behaviors of the four materials can be classified into two distinct groups. These are ductile materials, represented by steel and aluminum alloy, and brittle materials, represented by acrylic and WPC. For ductile materials, similar behavior of the AE signals was observed (Figures 2(a) and (b)). Based on the level of AE peak amplitude, the signals could be divided into three levels related to the failure behavior of ductile materials: an initial stage (low level of AE peak amplitude during elastic deformation and yield region), an intermediate stage (medium level of AE peak amplitude during the plastic deformation region), and a final stage (high level of AE peak amplitude during necking and final fracture). Notably, the AE signals detected from steel are denser than those from aluminum alloy.

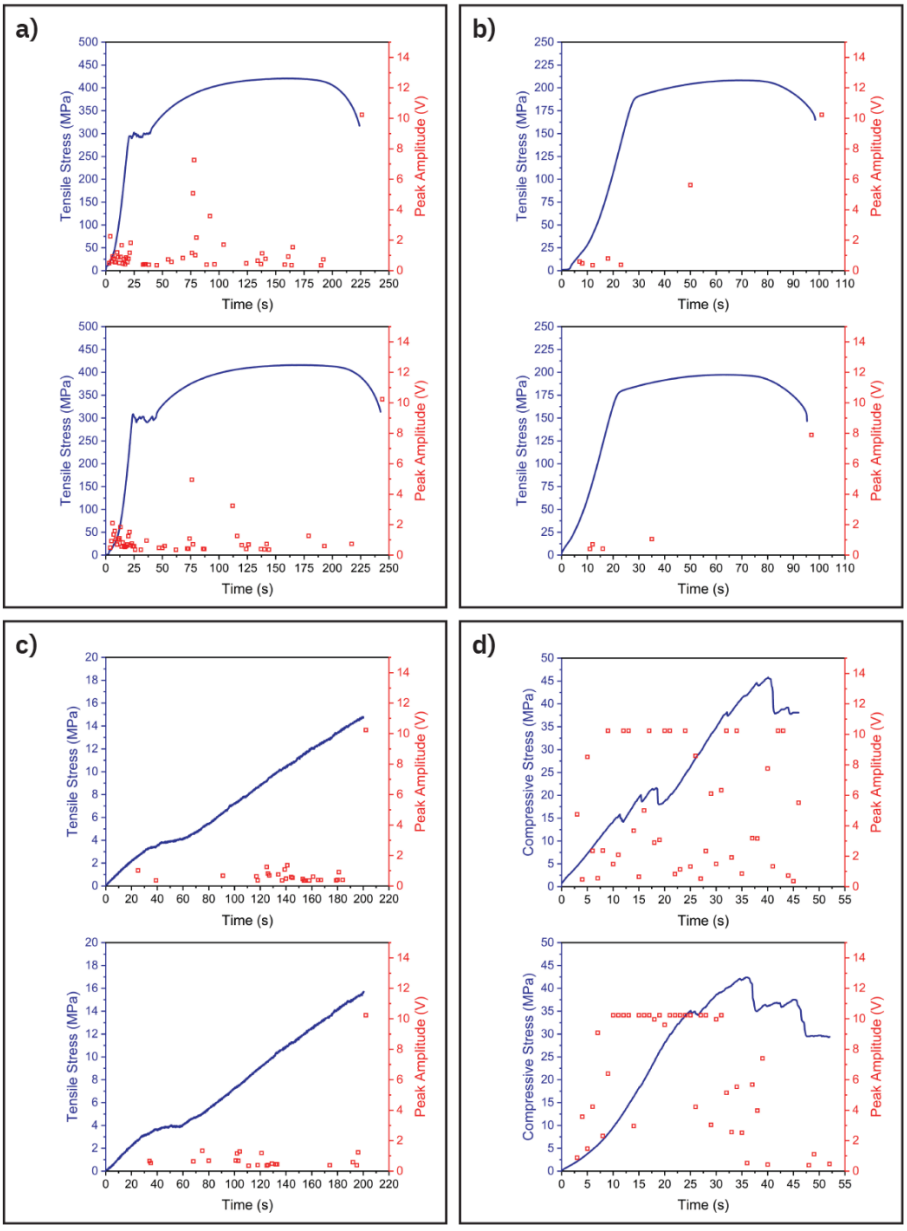

Figure 2 Stress–strain curves with AE signals for (a) steel, (b) aluminum alloy, (c) acrylic, and (d) WPC specimens

AE signals obtained from the steel specimens (Figure 2(a)) exhibit varying levels of peak amplitude at different stages of fracture. Multiple low AE peak amplitudes were recorded during the initial stage. The main AE signals exhibited peak amplitudes that were lower than 2 V. During plastic deformation, there was a consistent observation of a significantly increasing AE peak amplitude, ranging from 2 to 7 V, along with the presence of low AE peak amplitudes. In the final stage, specimen fracture, a noticeable increase in AE peak amplitude greater than 7 V was observed. In contrast, the amplitude of AE signals observed in aluminum alloy specimens (Figure 2(b)) was considerably lower compared to those observed in steel specimens. The AE signals were detected predominantly during the initial stage of the testing process. Few AE signals with very small peak amplitudes below 1 V were observed during the early stage. AE signals were rarely observed in the intermediate stage. A peak amplitude higher than 1 V was observed from some samples. In the final fracture stage, a considerable increase in AE peak amplitude, exceeding 7 V, was detected.

Normally, the peak amplitude of an AE signal is correlated with the intensity of the source within the material producing an acoustic emission [24, 25]. The initial low level of AE peak amplitudes reported during the initial stage would correspond to dislocation movement, localized deformation mechanisms, or micro-crack formation inside the material. The observed rise in AE peak amplitude during the intermediate stage suggests a higher intensity and energy release during plastic deformation. This would correspond to a continuing dislocation movement and the propagation of cracks inside the materials. The differences in magnitude and number of the AE signals produced from steel and aluminum alloy specimens can potentially be attributed to different crystal structures and mechanical properties, such as the modulus of elasticity, yield strength and tensile strength. The critical resolved shear stress (the stress required for dislocation) exhibits a magnitude approximately 100 times greater for the body-centered cubic (BCC) structures, such as steel, compared to the face-centered cubic (FCC) structures, such as aluminum alloy [26]. Consequently, this difference contributes to the elevated elastic modulus and yield stress observed in steel. The FCC structure has more slip planes and directions, which significantly enhance dislocation mobility. In contrast, the BCC structure, with its lower atomic packing factor (0.68) compared to the FCC structure (0.74), has fewer slip planes. This characteristic of the BCC structure restricts dislocation movement and inhibits crack propagation, leading to higher intensity AE signals in steel compared to aluminum alloys. Moreover, Mlikota and Schmauder [26] and Guo et al. [27] reported that aluminum alloy has low crack nucleation and work hardening rates compared to steel. Inferior crack nucleation and work hardening rates of aluminum alloy may result in reduced dislocation activity and hindered crack propagation, leading to a comparatively lower generation of AE signals. These identified characteristics may potentially contribute to a reduced intensity of AE signals that are observed in aluminum alloy. Finally, the high level of AE peak amplitudes observed in the final stage would correspond to the final fracture of the specimens.

The AE behaviors observed during uniaxial testing of brittle material specimens exhibited distinct differences compared to those observed for ductile materials, as shown in Figures 2(c) and (d). The stress-time curves predominantly displayed an almost linear deformation region. Fluctuating values of AE peak amplitude were observed throughout the test. The AE signals detected from acrylic are fewer in number and have lower peak amplitude compared to those from WPC. The AE signals for the acrylic specimens showed a low peak amplitude (less than 2 V) throughout tensile loading until a high peak amplitude (approximately 10 V) was observed at the point of final fracture. In contrast, the AE peak amplitude for the WPC specimen exhibited fluctuating values, between 0.35 V and 10 V, throughout compression testing. The increased number of signals and higher peak amplitude indicate a greater occurrence of AE events during the testing process, suggesting a higher level of internal damage and cracking within the WPC material. Low acoustic AE peak amplitudes detected in brittle materials suggest the initiation of micro-cracks. Additionally, high AE peak amplitudes detected at the end of acrylic testing would correspond to a final fracture. Furthermore, high levels of AE peak amplitudes detected in WPC would be consistent with the creation and propagation of macro-cracks resulting from continuous loading. AE behaviors have been reported for PMMA acrylic by Guo and Wong [9] and for cement paste by Anay et al. [21] and Gu et al. [22]. Guo and Wong [9] noted that detection of AE signals was challenging due to the relatively low occurrence of microcracks in the PMMA specimens. This difficulty may be attributed to the low tensile strength of pure PMMA [28]. Anay et al. [21] and Gu et al. [22] reported that AE signals detected primarily at the end of loading in cement paste were attributed to unstable crack formation and propagation of cracks. In contrast, AE signals related to micro-crack initiation were observed throughout the entire duration of the test.

3.2 Frequency domain analysis

Almost all detectable signals were processed using Fast Fourier Transform (FFT) analysis to clearly understand variations in signal frequencies related to the failure behavior of each type of specimen. The waveforms were selected from signals recorded at various stages of material damage, including peak amplitudes derived from duplicate data of ten tested samples for each specimen type. From the steel results (Figures 3(a) – (f)), AE signals and FFT spectra provide distinct indications of different stages in the deformation and fracture processes of steel specimens by analyzing AE peak amplitude, waveform characteristics, and the frequency range of the AE signals. Figures 3(a) and (b) show two typical waveforms and their corresponding AE signal frequency spectra obtained from steel specimens during the initial stage of tensile loading. The graphs in Figure 3(a), relating to the low AE peak amplitude of less than or equal to 1 V (lasting for approximately 0.4 ms), show a small broad peak in the FFT spectrum, with the most dominant frequency being around 225–275 Hz. AE peak amplitudes ranging between 1 and 2 V reveal two significant frequency bands, 25–75 kHz and 425–475 kHz, as shown in Figure 3(b). The signal length is approximately 0.6 ms. These two forms of AE signals and frequency spectra were also observed from AE signals with peak amplitudes below 2 V during the intermediate stage. Three typical waveforms and frequency characteristics of AE signals detected from steel specimens during the intermediate stage are depicted in Figures 3(c), (d) and (e). The quick attenuated signal, lasting less than 0.1 ms, with AE peak amplitude higher than 1 V was detected at this stage. The signals shown in this format did not have a notable frequency spectrum (Figure 3(c)). The signal displayed in Figure 3(d) demonstrates another set of characteristics, revealing a wide peak in the FFT spectrum with the most relevant frequencies between 250 and 350 kHz. The signals had amplitude peaks ranging from 2 to 3 V and duration of approximately 0.5 ms. Furthermore, the rapidly attenuated signals, lasting less than 0.2 ms with AE peak amplitudes greater than 3 V, were also detected at this stage. The broad frequency ranges between 25 and 150 kHz, with a maximum peak at around 50–60 kHz, are shown in Figure 3(e). The typical waveforms and frequency characteristics of AE signals observed during the final stage are depicted in Figure 3(f). Other signals were similar to those in the intermediate stage. Signals showing high peak amplitudes and relatively long continuous waveforms (>14 ms) were observed in the frequency range between 25 and 150 kHz, with the most notable frequencies at approximately 35 kHz.

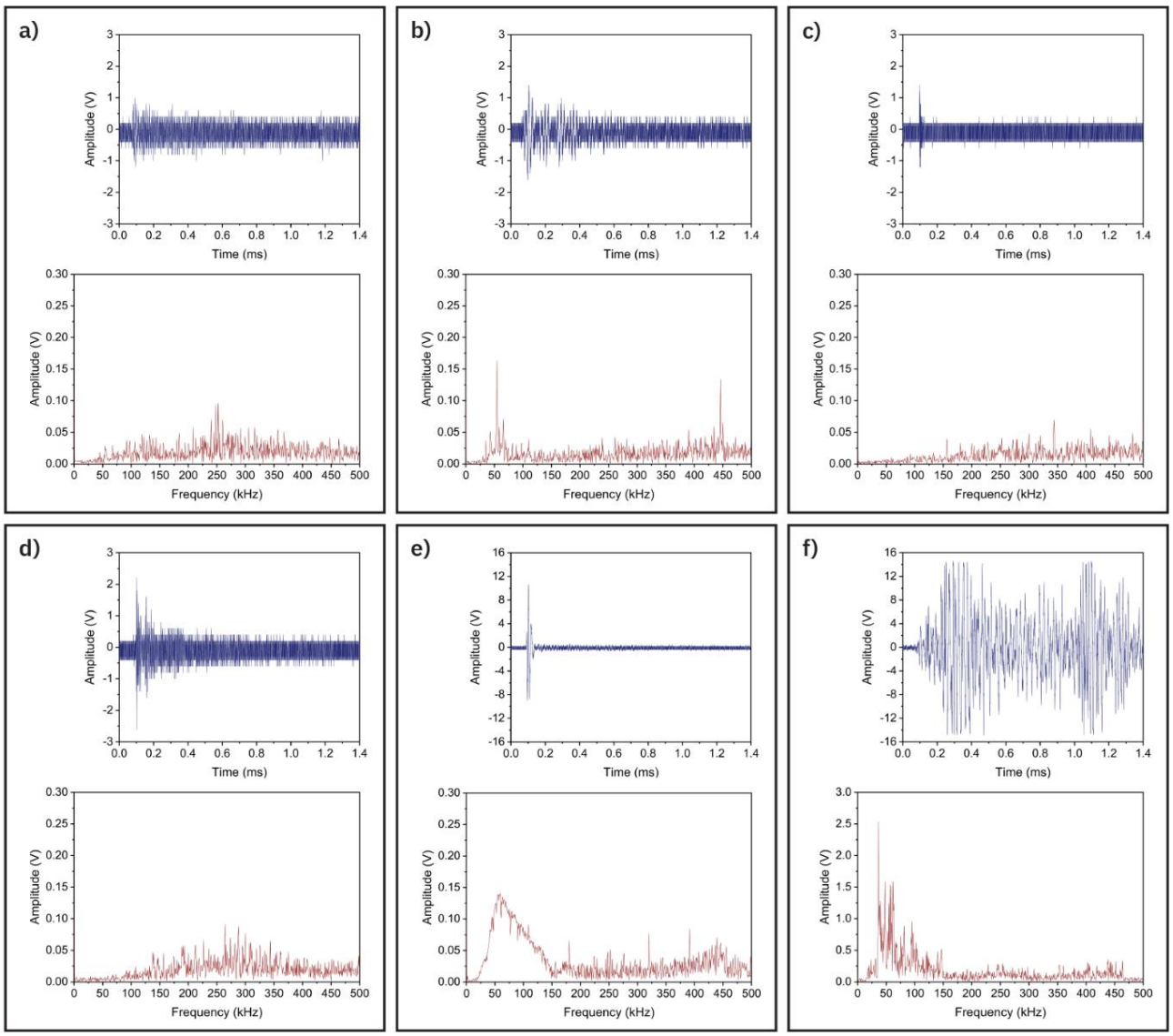

Figure 3 Typical AE waveforms and corresponding frequency spectra of AE signals of steel specimens during (a and b) the initial stage, (c, d and e) the intermediate stage and (f) the final stage of tensile loading

Selected typical AE signals along with their corresponding FFT spectra recorded from aluminum alloy specimens are presented graphically in Figures 4(a)–(c). The AE signals, along with the FFT spectra, also provided clear indications of different stages of aluminum alloy tensile behavior. According to the results, AE signals detected from aluminum alloy exhibited different characteristics and frequency spectra from those observed from steel. During the initial stage of the tensile testing, AE signals with low peak amplitudes of approximately 1 V (lasting up to 0.5 ms) were observed, as illustrated in Figure 4(a). These signals did not exhibit a dominant frequency spectrum. Two distinct frequency ranges are apparent, as shown in Figure 4(b), describing the behavior during the intermediate stage. The more prominent range was observed at 100–150 kHz, while less significant signals were observed at 350–400 kHz. The maximum peak amplitude was detected at about 6 V with a duration of around 1.0 ms. In the final stage, a signal with high peak amplitude, a relatively long continuous waveform (>1.4 ms) and a significant frequency range spanning 25 to 150 kHz was observed. The most significant frequency was seen at about 50 kHz, as depicted in Figure 4(c). These waveform and frequency characteristics were similar to those identified in steel at the final stage, but the most significant frequency was different.

Acrylic specimens revealed three characteristic AE signals and their corresponding FFT spectra (Figures 5(a–c)) from initial loading until specimen fracture. Initially, as depicted in Figure 5(a), a rapidly attenuated signal was observed, lasting less than 0.1 ms, with an AE peak amplitude ranging between 1 and 2 V. However, this signal did not exhibit a significant frequency spectrum. Also, the typical waveform had an AE peak amplitude within the range of 1 to 2 V, accompanied by a waveform length of approximately 0.6 ms. This waveform revealed the presence of several small frequency bands, as depicted in Figure 5(b). Last, at the final fracture, a high peak amplitude with a continuous signal lasting longer than 1.4 ms was detected. This signal exhibited a broad frequency range from 25 to 250 kHz with the most significant at about 40 kHz, as illustrated in Figure 5(c). Figures 6(a–c) depict selected typical AE signals and their corresponding FFT spectra obtained from WPC specimens. Peak amplitudes of varying sizes, lasting approximately 0.6–0.8 ms, were detected throughout the testing. The signals exhibit similar patterns in their FFT spectra, encompassing several frequency ranges. However, distinctive variations in peak intensity can be observed in each frequency range. AE signal characteristics and failure stages during uniaxial testing of low-carbon steel, aluminum alloy, acrylic and WPC are summarized in Table 1.

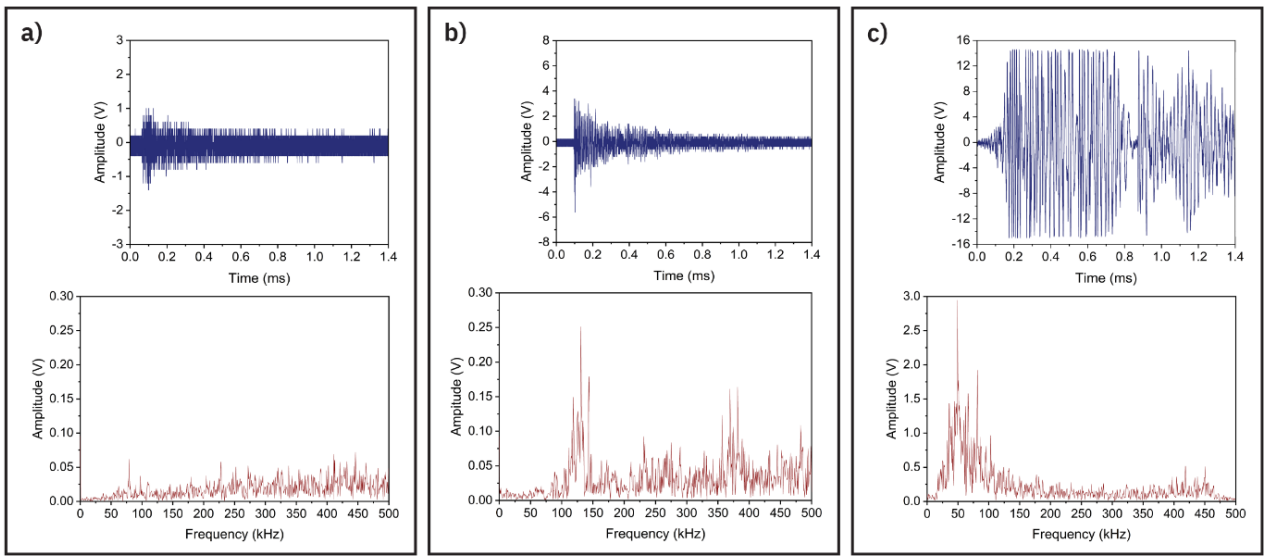

Figure 4 Typical AE waveforms and corresponding frequency spectra of AE signals of aluminum alloy specimens during (a) the initial stage, (b) the intermediate stage and (c) the final stage of tensile loading

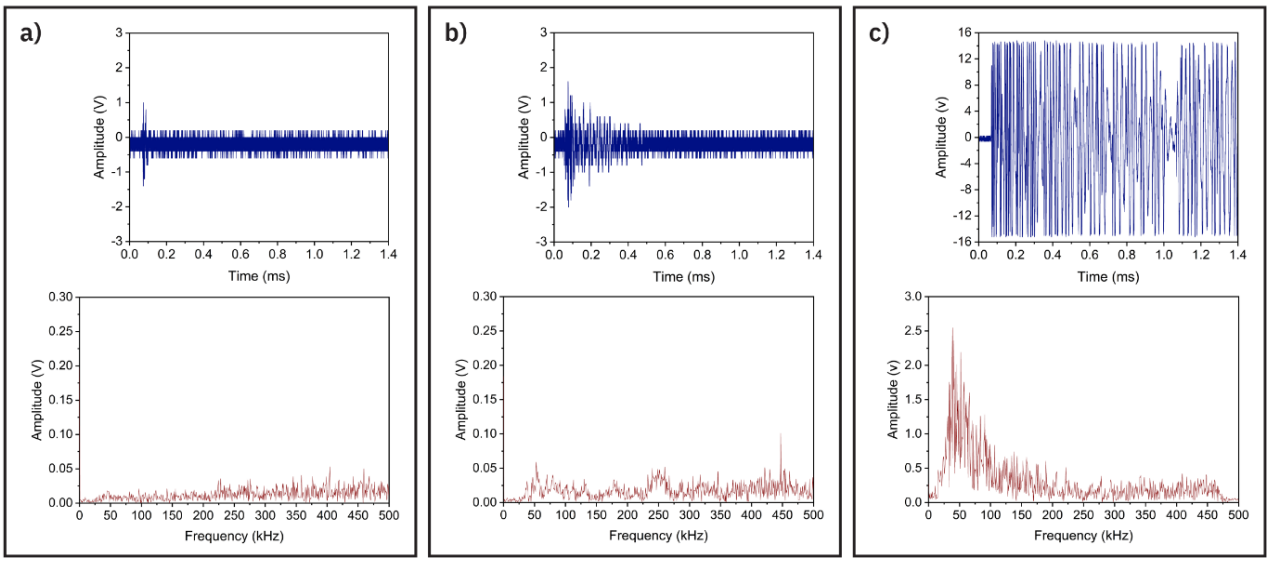

Figure 5 Three typical AE waveforms and corresponding frequency spectra of AE signals obtained from acrylic specimens during tensile loading

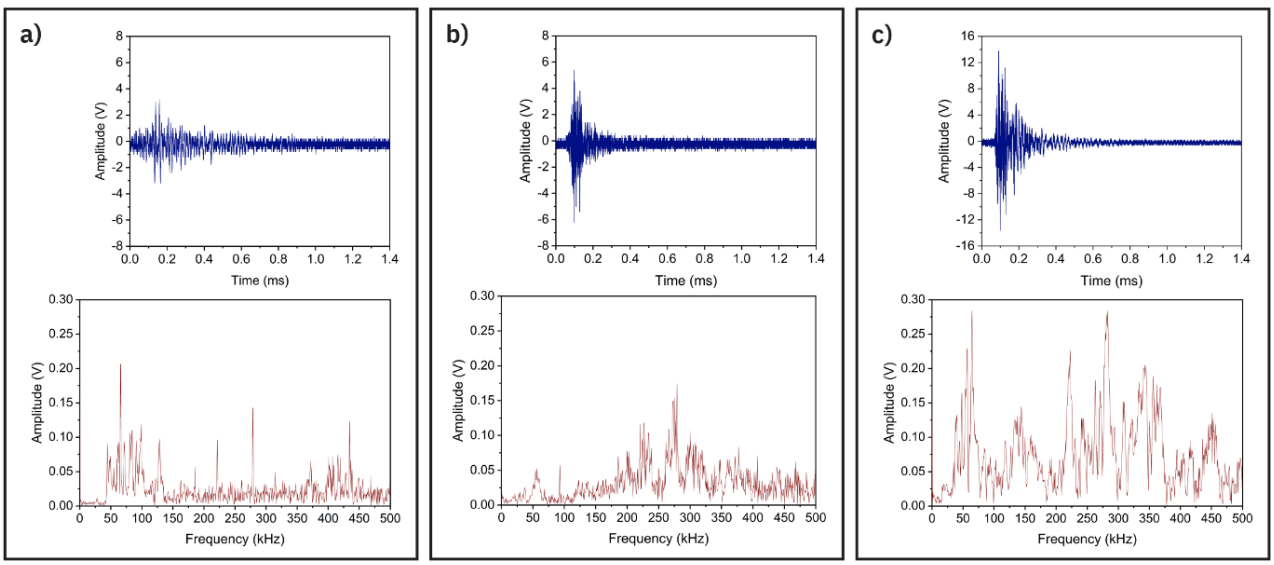

Figure 6 Three typical AE waveforms and corresponding frequency spectra of AE signals obtained from WPC specimens during compression loading

Table 1 Summary of AE signal characteristics and failure stages during uniaxial testing of low-carbon steel, aluminum alloy, acrylic and WPC.

Material	Failure stage	AE Peak amplitude (V)	Signal duration (ms)	Frequency range (kHz)
Ductile materials				
Low-carbon steel	Initial	≤ 1	~ 0.4	225–275
		1–2	~ 0.6	25–75, 425–475
	Intermediate	> 1	< 0.1	No notable spectrum
		2–3	~ 0.5	250–350
		> 3	< 0.2	25–150 (peak: 50–60)
	Final	High (> 10)	> 14	25–150 (peak: ~35)
Aluminum alloy	Initial	~1	≤ 0.5	No dominant frequency spectrum
	Intermediate	Up to 6	~ 1.0	100–150, 350–400
	Final	High (> 10)	> 1.4	25–150 (peak: ~50)
Brittle materials				
Acrylic	Linear deformation	1–2	< 0.1	No dominant frequency spectrum
		1–2	~ 0.6	Several small bands
	Final	High (> 10)	> 1.4	25–250 (peak: ~40)
WPC	All Stages	Varying	0.6–0.8	Several frequency ranges, with variations in peak intensity

In summary, the dissimilarity observed in the characteristic AE signals and their corresponding FFT spectra during each stage of failure behavior in individual materials may be related to distinct deformation and failure mechanisms inherent to the respective materials, as discussed in the previous section. From the overall analysis of the four tested materials, small AE peak amplitudes (<3 V) with higher AE frequency peaks (>200 kHz) are associated with the initial damage stages in ductile materials, while higher AE peak amplitudes (>3 V) with lower AE frequency peaks (25–150 kHz) correspond to the middle damage and the final fracture stages in both ductile and brittle materials. This trend can be attributed to the nature of the fracture mechanisms occurring at different stages of deformation. In ductile materials such as low-carbon steel and aluminum alloy, localized or minor damage tends to emit higher-frequency AE signals, whereas larger-scale damage (such as crack propagation or final fracture) shifts the spectrum toward lower frequencies due to longer-wavelength energy dissipation. In brittle materials like acrylic, no dominant frequency spectrum is observed initially; however, lower frequency bands emerge at final fracture, with peaks appearing around 40 kHz. In contrast, WPC exhibits multiple frequency peaks throughout all failure stages, indicating a more complex fracture pattern. The results show that AE signal data and its corresponding frequency spectra have potential for the prediction of failure stages and identification of material sources. The specimen material plays a critical role in determining the range of the AE signal frequency spectrum. Variations in intrinsic mechanical properties, microstructural characteristics, and failure mechanisms significantly influence the observed frequency ranges. For example, ductile materials often exhibit clear and well-defined peaks, occasionally presenting multiple dominant frequency bands depending on the failure stage. In contrast, brittle materials produce less distinct frequency spectra, with fewer dominant peaks, although specific bands become more noticeable in the final stage. In addition to material properties, variations in experimental conditions, such as tensile or compressive loading, could significantly affect the characteristics of the AE signal frequency spectrum. Tensile loading predominantly induces microcrack initiation and propagation, producing AE signals with distinct frequency peaks associated with these fracture mechanisms. In contrast, compressive loading generates AE signals related to mechanisms such as frictional sliding, crack formation, or pore collapse, potentially leading to multiple overlapping frequency spectra. However, further investigation is needed, particularly in the context of multi-material structures, to enhance the system's accuracy and applicability across different materials. This will help in better understanding the diverse failure mechanisms and improve the predictive capabilities of AE monitoring.

4. Conclusions

Based on AE signal monitoring and evaluation during uniaxial testing of low–carbon steel, aluminum alloy, PMMA acrylic and WPC specimens, the findings of this study can be summarized as follows:

1. The characteristics of AE peak amplitude detected during uniaxial testing differ among materials and are closely associated with their type, deformation mechanisms, and fracture behaviors. In ductile materials, steel and aluminum alloy, AE peak amplitude intensity distinctly identifies the regions of elasticity, plasticity, and fracture. Conversely, PMMA acrylic and WPC display fluctuating AE peak amplitudes throughout the linear deformation region, reflecting their unique fracture characteristic in brittle materials.
2. The diversity in the magnitude and number of AE signals generated during uniaxial testing was influenced by various factors, including crystal structure, failure behavior, mechanical strength, type of material and loading direction.
3. Analyzing the peak amplitude intensity and corresponding frequency spectrum of AE signals could offer distinct indications of failure behaviors in different materials, including specific behaviors in metal materials such as elastic and plastic deformations, as well as final fracture. This analytical approach allows precise identification of the fracture behavior exhibited by different materials.

5. Acknowledgements

This research work was supported by Research of Khon Kaen University and the Research Fund of the Faculty of Engineering, Khon Kaen University under the Research Scholarship for M. Eng. student projects under Contract M-Eng.-MME-001/2564.

6. References

[1] Calabrese L, Proverbio E. A review on the applications of acoustic emission technique in the study of stress corrosion cracking. Corros Mater Degrad. 2020;2(1):1-30.

[2] Kongpuang M, Culwick R, Cheputeh N, Marsh A, Jantara Junior VL, Vallely P, et al. Quantitative analysis of the structural health of railway turnouts using the acoustic emission technique. Insight Non-Destr Test Cond Monit. 2022;64(7):398-403.

[3] Topolář L, Kocáb D, Pazdera L, Vymazal T. Analysis of acoustic emission signals recorded during freeze-thaw cycling of concrete. Materials. 2021;14(5):1230.

[4] Shanbhag VV, Pereira PM, Rolfe FB, Arunachalam N. Time series analysis of tool wear in sheet metal stamping using acoustic emission. J Phys: Conf Ser. 2017;896:012030.

[5] Skåre T, Krantz F. Wear and frictional behaviour of high strength steel in stamping monitored by acoustic emission technique. Wear. 2003;255(7-12):1471-9.

[6] Laonapakul T, Nimkerdphol AR, Otsuka Y, Mutoh Y. Failure behavior of plasma-sprayed HAp coating on commercially pure titanium substrate in simulated body fluid (SBF) under bending load. J Mech Behav Biomed Mater. 2012;15:153-66.

[7] Jayakumar T, Mukhopadhyay CK, Venugopal S, Mannan SL, Raj B. A review of the application of acoustic emission techniques for monitoring forming and grinding processes. J Mater Process Technol. 2005;159(1):48-61.

[8] Abo-El-Ezz AE. Acoustic emission detection of micro-cracks initiation and growth in polymeric materials. In: Hassan MF, Megahed SM, editors. Current Advances in Mechanical Design and Production VII. Oxford: Elsevier; 2000. p. 253-60.

[9] Guo TY, Wong LNY. Cracking mechanisms of a medium-grained granite under mixed-mode I-II loading illuminated by acoustic emission. Int J Rock Mech Min Sci. 2021;145:104852.

[10] Ríos-Soberanis CR, Wakayama S, Sakai T, Cervantes-Uc JM, May-Pat A. Evaluation of mechanical behaviour of bone cements by using acoustic emission technique. Adv Mater Res. 2014;856:246-50.

[11] Roques A, Browne M, Thompson J, Rowland C, Taylor A. Investigation of fatigue crack growth in acrylic bone cement using the acoustic emission technique. Biomaterials. 2004;25(5):769-78.

[12] Xu Y, Mellor BG. Characterization of acoustic emission signals from particulate filled thermoset and thermoplastic polymeric coatings in four point bend tests. Mater Lett. 2011;65(23-24):3609-11.

[13] Loanapakul T, Otsuka Y, Mutoh Y. Fatigue and acoustic emission behavior of plasma sprayed HAp top coat and HAp/Ti bond coat with HAp top coat on commercially pure titanium. Key Eng Mater. 2011;452-453:857-60.

[14] Laonapakul T, Otsuka Y, Nimkerdphol AR, Mutoh Y. Acoustic emission and fatigue damage induced in plasma-sprayed hydroxyapatite coating layers. J Mech Behav Biomed Mater. 2012;8:123-33.

[15] Kongpuang M. Reliability-base monitoring and maintenance of urban railway turnout using acoustic emission [dissertation]. Birmingham: University of Birmingham; 2022.

[16] Zhao Y, Zhang Y, Xu J, Zhang M, Yu P, Zhao Q. Frequency domain analysis of mechanical properties and failure modes of PVDF at high strain rate. Constr Build Mater. 2020;235:117506.

[17] Vetrone J, Obregon JE, Indacochea EJ, Ozevin D. The characterization of deformation stage of metals using acoustic emission combined with nonlinear ultrasonics. Measurement. 2021;178:109407.

[18] Behrens BA, Hübner S, Wölki K. Acoustic emissions during tensile test of DC06 and HCT600X. Mater Sci Eng Technol. 2019;50(7):796-809.

[19] Pattnaik AB, Das S, Jha BB, Prasanth N. Effect of Al–5Ti–1B grain refiner on the microstructure, mechanical properties and acoustic emission characteristics of Al5052 aluminium alloy. J Mater Res Technol. 2015;4(2):171-9.

[20] Vanniamparambil PA, Guclu U, Kontsos A. Identification of crack initiation in aluminum alloys using acoustic emission. Exp Mech. 2015;55:837-50.

[21] Anay R, Soltangharaei V, Assi L, DeVol T, Ziehl P. Identification of damage mechanisms in cement paste based on acoustic emission. Constr Build Mater. 2018;164:286-96.

[22] Gu Q, Ma Q, Tan Y, Jia Z, Zhao Z, Huang D. Acoustic emission characteristics and damage model of cement mortar under uniaxial compression. Constr Build Mater. 2019;213:377-85.

[23] Japanese Industrial Standard. JIS Z 2201:1998 Test pieces for tensile test for metallic materials. Tokyo: JIS; 1998.

[24] Ono K. Application of acoustic emission for structure diagnosis. Diagnostyka. 2011;2(58):3-18.

[25] Hase A, Mishina H, Wada M. Correlation between features of acoustic emission signals and mechanical wear mechanisms. Wear. 2012;292-293:144-50.

[26] Mlikota M, Schmauder S. On the critical resolved shear stress and its importance in the fatigue performance of steels and other metals with different crystallographic structures. Metals. 2018;8(11):883.

[27] Guo Y, Paramatmuni C, Avcu E. Void nucleation and growth from heterophases and the exploitation of new toughening mechanisms in metals. Crystals. 2023;13(6):860.

[28] Naznin H, Mallik AK, Hossain KS, Shahruzzaman MD, Haque P, Rahman MM. Enhancement of thermal and mechanical properties of PMMA composites by incorporating mesoporous micro-silica and GO. Results Mater. 2021;11:100203.